International Journal of Multidisciplinary Research and Growth Evaluation.

# *In vitro* experiments and transcriptomic analysis reveal the antibacterial mechanism of coptisine against Aeromonas veronii

**Ziyan Yang [1], Daiqin Yang [2], Mengting Pei [3], Pupu Yan [4], Rong Li [5], Meilin Qin [6], Yiman Du [7], Yan Zhang [8], Yumeng Ban [9], Hanfei Wang [10], Feng Chen [11], Liwei Guo [12], Yingbing Su [13*]**
[1-13] College of Animal Science and Technology, Yangtze University, Jingzhou 434025, China

* Corresponding Author: **Yingbing Su**

## Article Info

**ISSN (Online):** 2582-7138
**Impact Factor (RSIF):** 8.04
**Volume:** 07
**Issue:** 02
**March-April 2026**
**Received:** 17-02-2026
**Accepted:** 15-03-2026
**Published:** 13-04-2026
**Page No:** 610-618

**Abstract**
To investigate the inhibitory effect of coptis alkaloid on the growth of *Aeromonas veronii* and its mechanism. The minimum inhibitory concentration (MIC) was determined by the microbroth dilution method; A growth curve was plotted to evaluate the bacteriostatic kinetics; Morphology of the cells was observed by transmission electron microscopy; The formation of biofilms was determined by crystal violet staining; Kits detect alkaline phosphatase (AKP) and protein leakage; Transcriptome sequencing of bacteria treated with coptis alkaloid, screening for differentially expressed genes, and GO and KEGG enrichment analysis; RT-qPCR was used to validate the sequencing results. The MIC of coptis alkaloid against *Aeromonas veronii* was 40 μg/mL. At 1MIC concentration, coptisine significantly inhibited bacterial growth, disrupted cell morphology, and inhibited biofilm formation. AKP and protein leakage increased significantly with the increase of coptis alkine concentration, indicating impaired cell wall/membrane integrity. Transcriptome analysis identified a total of 171 DEGs (87 up-regulated and 84 down-regulated), and KEGG enrichment analysis showed that the differentially expressed genes were significantly enriched in glycerophospholipid metabolism, PPAR signaling pathway, nucleotide metabolism, purine metabolism and other pathways. RT-qPCR verification results were consistent with sequencing data. Coptisine exerts antibacterial effects through multiple pathways such as disrupting the cell wall/membrane structure of *Aeromonas veronii*, inhibiting biofilm formation, and interfering with energy metabolism.

**Keywords:** Coptisine, Aeromonas veronii, Bacteriostatic, Transcriptome analysis

## 1. Introduction

*Aeromonas veronii* is a Gram-negative facultative anaerobic bacterium of the genus Aeromonas in the Vibriaceae family. It is an important zoonotic pathogen that is widely distributed in various aquatic environments and poses a significant threat[1, 2] to public health and aquaculture. In recent years, its growing problem of drug resistance has become one of the main factors restricting the healthy development of aquaculture and has caused huge economic losses[3]. At present, antibiotics remain the main means[4] of preventing and treating infections caused by this bacterium. However, the long-term and excessive use of antibiotics can not only lead to increased drug resistance in strains but also cause a series of problems such as weakened host immune function, water pollution and ecological balance disruption.[5] Therefore, the development of efficient, safe and environmentally friendly alternatives to antibiotics has become an urgent need in the field of aquatic disease control.

Chinese herbal medicines and their monomer compounds have multiple advantages such as antibacterial, anti-inflammatory, immunity-boosting, low residue and low resistance, showing great potential[6, 7] as alternatives to antibiotics. Studies have shown that scientifically formulated Chinese herbal preparations can not only effectively prevent and treat diseases, but also promote animal growth[8, 9], improve the body's anti-stress ability[10], increase feed utilization[11], and enhance product quality[12], Coptis chinensis is an important component of many classic prescriptions, Its core active ingredient, the alkaloid coptisine (a type of

isoquinoline alkaloid), has been proven to have broad-spectrum pharmacological activities[13, 14] such as antibacterial, antiviral, anti-inflammatory and antioxidant. However, the specific inhibitory effect and detailed mechanism of coptisine against *Aeromonas veronii* have not been systematically reported. In view of this, the present study explored the inhibitory effect of coptisine on *Aeromonas veronii* through *in vitro* experiments combined with transcriptomic sequencing, and preliminarily clarified its antibacterial mechanism using bioinformatics analysis. This study aims to provide a theoretical basis for developing novel coptisine-based antibacterial agents for aquaculture.

## 2. Materials

### 2.1. Strain and culture

*Aeromonas veronii* was provided by Prof. Fuxian Zhang (College of Animal Science and Technology, Yangtze University). The strain was stored in LB medium containing 50% glycerol and frozen at -80 ℃. Before experiments, the strain was streaked onto LB solid plates and incubated at 37 °C overnight. Single colonies were inoculated into LB liquid medium and cultured to logarithmic phase for subsequent use.

### 2.2. Reagents and instruments

Coptisine (purity > 95%) was purchased from Shanghai Maclean Biochemical Technology Co., Ltd. Other reagents included dimethyl sulfoxide (DMSO), BCA protein assay kit, tryptone, NaCl, and AKP assay kit. Major instruments included a microplate reader, autoclave, ultrapure water system, transmission electron microscope, and constant temperature shaker.

### 2.3. Determination of minimum inhibitory concentration (MIC)

The microbroth dilution method was used to determine the MIC of coptisine against *Aeromonas veronii*. The stock solution was prepared by dissolving the coptisine powder with DMSO. In 96-well plates, continuous double dilution of coptisine with Mueller-Hinton broth medium results in final concentration gradients of 20, 40, 80, and 160 μg/mL, respectively. Subsequently, equal volumes of bacterial liquid ($1.0\times10^8$ CFU/mL) were added to each well. Positive control Wells (containing only the bacterial liquid and medium) and solvent control Wells (containing equal volumes of DMSO, bacterial liquid and medium) were set up simultaneously. After culturing at 37℃ for 24 hours, the bacterial growth in each well was observed with the naked eye. The minimum drug concentration at which no obvious bacterial growth was observed with the naked eye was the MIC.

### 2.4. Determination of the growth curve of *Aeromonas veronii*

Dilute *Aeromonas veronii* PBS in the logarithmic growth phase to a concentration of $1.0\times10^8$ CFU/mL. Inoculated into LB liquid medium containing different concentrations of coptis alkaloid (1/16, 1/8, 1/4, 1/2, 1×MIC). Equal volumes of PBS treated culture medium were set as the blank control and DMSO treated culture medium as the negative control. All samples were incubated in a constant temperature shaker at 37 ℃ and 150 rpm. Shake and incubate at 37 ℃, 150 rpm, take samples at 0, 2, 4, 6, 8, 10, 12, 14 h, measure OD600 values, and plot growth curves. Three replicates were set for each group.

### 2.5. Effects of coptisine on the cell wall of *Aeromonas veronii*

The coptisine solution was added to the *Aeromonas veronii* suspension at a final concentration of $1.0\times10^8$ CFU/mL, with the final concentrations of action being 1/4 MIC, 1/2 MIC, and 1 MIC respectively, and blank controls treated with equal volumes of PBS and negative controls treated with equal volumes of DMSO were set up. All samples were placed in a 37 ℃, 150 rpm constant temperature shaking incubator for shaking culture. Samples were taken after culturing for 0, 2, 4, and 6 hours respectively, and then centrifuged at 1000-1500 rpm for 10 minutes to collect the supernatant. The samples were processed according to the instructions of the alkaline phosphatase (AKP) test kit, and the absorbance was measured at a wavelength of 520 nm using an enzyme-linked immunosorbent assay (ELISA) reader to calculate the AKP activity in each group of culture supernatants at different time points.

### 2.6. Determination of biofilm formation of *Aeromonas veronii* by coptis alkaloid

The biofilm was quantitatively determined using crystal violet staining. *Aeromonas veronii* was cultured to the logarithmic growth phase, the cells were collected and washed three times with PBS, resuspended and the suspension concentration was adjusted to $1.0\times10^8$ CFU/mL. Inoculated at this concentration into LB media containing 1/4 MIC, 1/2 MIC and 1 MIC of coptisine, with solvent control groups containing equal volumes of DMSO and blank control groups containing only the medium. The culture was carried out in 24-well cell culture plates, with 1 mL of the corresponding medium added to each well, and placed at 37 ° C for aerobic culturing for 24 hours.

After culturing, discard the supernatant from each well and wash the Wells three times with PBS to remove airborne bacteria. Add 500 μL of 99% methanol to each well and fix in an oven at 60 ° C for 30 minutes. Discard the fixative and wash three times with PBS. Add 1% crystal violet staining solution to each well and shake at 120 rpm at room temperature for 30 minutes. Discard the staining solution after staining, wash with PBS until the background is colorless, and aspirate the remaining liquid. Place the plate in a 37 ° C oven to dry for 30 minutes. After drying, add 500 μL of 30% glacial acetic acid solution to each well and shake at 150 rpm for 15 min to fully dissolve the crystalline purple - biofilm complex bound to the bottom of the well. Finally, draw the dissolution from each well into a 96-well plate and measure the absorbance at a wavelength of 570 nm using an enzyme-linked immunosorbent assay reader.

### 2.7. Determination of protein content in *Aeromonas veronii* by coptis alkaloid

Collect *Aeromonas veronii* in the growth logarithmic phase, resuspend them after washing with PBS, and adjust the suspension concentration to $1.0\times10^8$ CFU/mL. Inoculate the cultures into LB liquid media containing final concentrations of 1/4 MIC, 1/2 MIC and 1 MIC of coptisine, and set up solvent control groups treated with equal volumes of DMSO and blank control groups without drug addition. All treatment groups were incubated in a constant temperature shaking incubator at 37 ° C and 200 rpm. After culturing for 2, 4, 6, 8, and 10 hours respectively, 5 μL of bacterial liquid was taken from each treatment group and treated according to the instructions of the BCA protein concentration assay kit. The

absorbance values of each sample were measured at a wavelength of 595 nm using an enzyme-linked immunosorbent assay (ELISA) reader, and the protein content in the cells at the corresponding time points was calculated based on the standard curve.

**2.8. Transcriptome sequencing sample preparation**

Determine the growth pattern of *Aeromonas veronii* by measuring the growth curve. Subsequent processing is carried out when the bacterial liquid enters the logarithmic growth phase. Transfer the activated bacteria to fresh LB medium and adjust the bacterial suspension concentration to $1\times10^{10}$ CFU/mL. Subsequently, coptisine solution was added to the experimental group's bacterial liquid to make the final concentration 1×MIC; An equal volume of DMSO solvent was added to the control group. Transfer the treated bacterial liquid to a 1.5 mL sterile capped centrifuge tube and centrifuge at 5000 × g for 5 minutes at 4 ° C. Carefully discard the supernatant and collect the bacterial precipitate. Quickly place the cryotubes containing the bacterial precipitate in dry ice to ensure RNA integrity and proceed with subsequent RNA extraction and transcriptome sequencing.

**2.9. Transcription library formation and sequencing**

rRNA was removed using the RiboCop rRNA Depletion Kit for Mixed Bacterial Samples (lexogen, USA), and mRNA was randomly broken into small fragments of about 200bp using mRNA as a template. Double-stranded cDNA was synthesized by reverse transcription using random primers. When synthesizing the second strand of cDNA, dUTP was used instead of dTTP for synthesis. The synthesized double-stranded cDNA was added to End Repair Mix to fill the flat end, phosphorylated at the 5 'end, and an A base was added to the 3' end to link the Y-shaped sequencing linker. The second strand of cDNA containing dUTP was then eliminated with the UNG enzyme, resulting in the library containing only the first strand of cDNA. RNA library construction was performed using Illumina® Stranded mRNA Prep Ligation from Illumina (San Diego, CA). Perform RNA-seq double-ended sequencing using an illumina sequencer (NovaSeq6000 or other new model).

**2.10. Sequencing data quality control assessment**

The Illumina platform converts sequencing image signals into text signals through CASAVA Base Calling and stores them in fastq format as raw data. Remove adapter sequences from reads; Shear out the 5 'end that contains non-A, G, C, T bases; Trim the ends of reads with lower sequencing quality (sequencing quality values less than Q20); Remove reads with a proportion of N reaching 10%; Discard small fragments that are less than 25bp in length after adapter removal and quality trimming. The high-quality reads obtained after the above series of quality cuts are called clean data.

**2.11. Enrichment analysis of differential genes (DEGs)**

Differential expression analysis was performed using DESeq2 software, with the screening criteria being $\log_2$(Fold Change) $\geq 1$ and $P \leq 0.05$. GO functional annotation and KEGG pathway enrichment analysis were performed on the differentially expressed genes.

**2.12. RT-qPCR validation**

After activation and dilution of *Aeromonas veronii*, a 1×MIC coptisine drug was used to set up a control group. The specific experimental procedures were the same as 2.7. After RNA extraction, it was immediately reverse transcribed into cDNA and detected using SYBRGreen I chimeric fluorescence. The detection was based on the relevant sequences of *Aeromonas veronii* provided in the database of Meiji Bio Company, with the 16S rRNA gene as the internal reference. Four replicates were set up in the experiment. Primer design was performed using Primer Premier5 software, and the primers were synthesized by Bioengineering (Shanghai) Co., LTD. Information on the screened gene primers is shown in Table The relative expression levels of the target genes were calculated using method $2^{-\triangle\triangle Ct,}$ and the differences among the groups of data were analyzed by t-test.

**3. Results and Analysis**

**3.1. Minimum inhibitory concentration of coptis alkaloid against *Aeromonas veronii***

The results are shown in Figure 1. When *Aeromonas veronii* was treated with 40, 80, 160, 320 μg/mL of coptisine, it was found that the medium was clear and transparent when 80 μg/mL of coptisine was added to the same volume of bacterial liquid, indicating that the minimum inhibitory concentration of coptisine against *Aeromonas veronii* was 40 μg/mL.

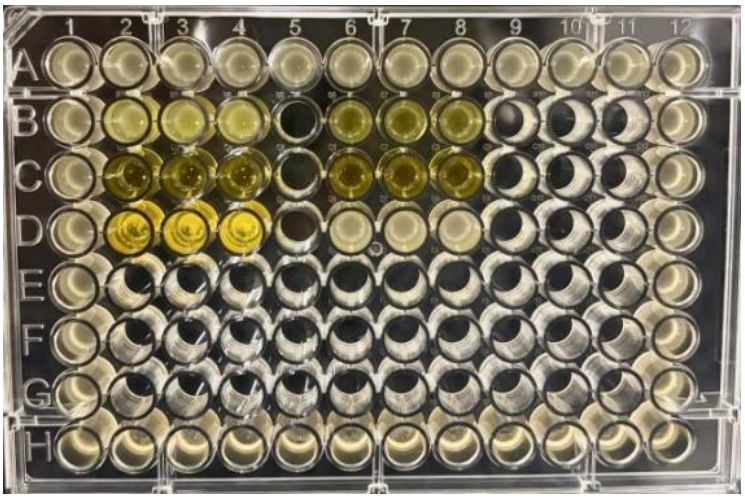


**Fig 1:** Determination of the minimum inhibitory concentration of coptis alkaloid against *Aeromonas veronii*

### 3.2. The effect of coptisine on the growth curve of *Aeromonas veronii*

The result is shown in Figure 2. When the concentration of coptisine was 1/16 MIC, no significant inhibitory effect was observed on the growth of *Aeromonas veronii*; When the concentration reached 1 MIC, coptisine significantly inhibited bacterial growth and delayed the point when the strain entered the logarithmic growth phase. The results suggest that coptisine has an inhibitory effect on *Aeromonas veronii* in a concentration-dependent manner.

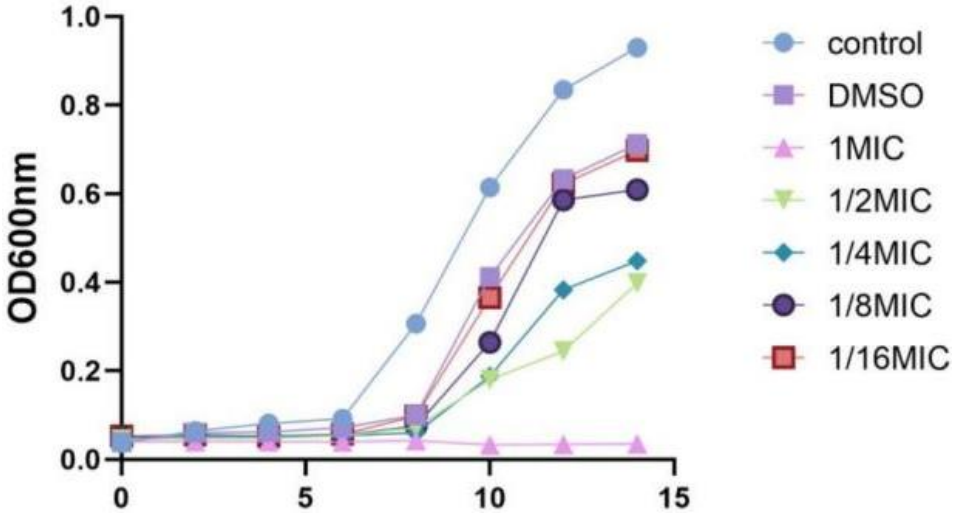


**Fig 2:** Growth curves of *Aeromonas veronii* at different concentrations of coptis alkaloids

### 3.3. Effects of coptisine on the cell wall of *Aeromonas veronii*

Alkaline phosphatase is an active enzyme that exists between the cell wall and cell membrane of bacteria. When the bacterial cell structure is intact, the extracellular content of alkaline phosphatase is low, but when the cell wall is damaged, intracellular alkaline phosphatase is released extracellular, so it is often used as one of the indicators to judge whether the cell wall structure is intact. As shown in Figure 3, there is no difference between the blank group and the DMSO group ($P>0.05$); Meanwhile, the blank group showed a significant difference ($P< 0.05$) compared with the 1/4MIC group and a significant difference ($P<0.01$) compared with the 1MIC group. During the 0, 2, 4, and 6 hours periods, the AKP content was relatively stable and increased in a dose-dependent manner with the increase of coptisine concentration. It indicates that coptisine destroys the cell wall structure of *Aeromonas veronii*.

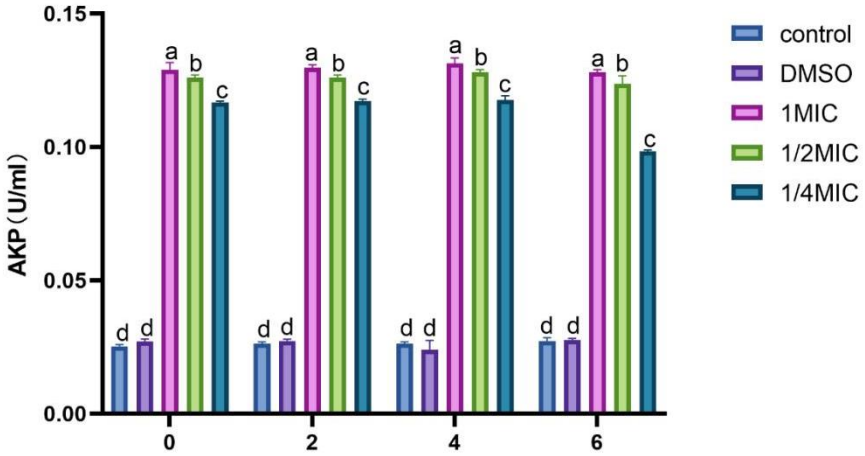


**Fig 3:** Influence of coptisine at different concentrations on AKP content of *Aeromonas veronii*

### 3.4. Effects of coptisine on biofilm formation of *Aeromonas veronii*

The biofilms were determined by crystal violet staining to evaluate the effects of different concentrations of coptis alkaloid on the formation of biofilms of Aeromonas vensii. The results, as shown in Figure 4, showed no difference between the blank group and the DMSO group ($P>0.05$); The different concentrations of coptisine treatment were significantly lower than the blank group at OD570nm ($P< 0.05$) ($P<0.01$), and showed a dose-dependent decrease. These results suggest that coptisine can inhibit the formation of *Aeromonas veronii* biofilms.

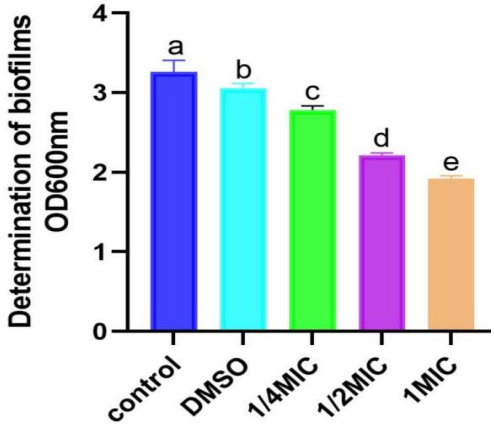


**Fig 4:** Effects of coptisine at different concentrations on AKP content of *Aeromonas veronii*

### 3.5. Effects of coptisine on the proteins of *Aeromonas veronii*

The protein content of Aeromonas victori treated with different concentrations of coptisine for 8 hours was detected using a kit, as shown in Figure 5. In the blank group without coptisine treatment, the protein content in the bacterial supernatant was lower. Compared with the blank group, after 8 hours of coptisine treatment, 1MIC and 1/2MIC concentrations of coptis chinensis significantly increased protein content ($P<0.05$), while no significant difference was found in the DMSO group. After 8 hours of treatment with coptisine, the integrity of the cell membrane and cell wall of *Aeromonas veronii* was disrupted, resulting in the release of proteins from extracellular to extracellular, thereby affecting protein synthesis.

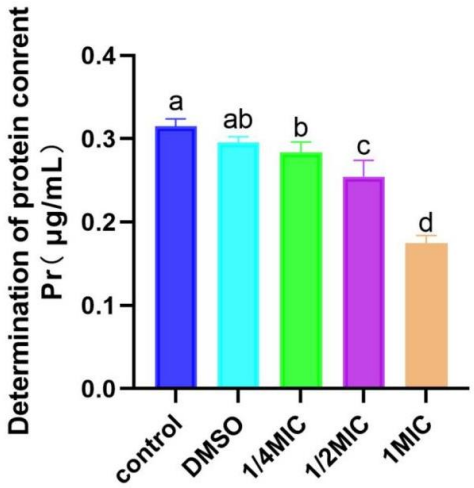


**Fig 5:** Effect of coptisine at different concentrations on the protein of *Aeromonas veronii*

### 3.6. Sequencing data quality control analysis

Six target sample libraries were constructed and sequenced on the machine. The data quality control results are shown in the table 1. The treatment group (AV_Y1 group) and the control group (AV group) obtained an average of 23,233,672 valid sequences and 24,434,176 valid sequences respectively. In addition, the base error rate of each sample in both the control group and the treatment group was 0.0117. Among them, the base mass values Q20 (with an average accuracy rate of 99.43% for identifying bases) and Q30 (with an average accuracy rate of 96.34% for identifying bases) were above 99.32% and 96.34% respectively. This indicates that the Raw reads obtained from sequencing, as well as the filtered clean reads, meet the quality control requirements and are suitable for bioinformatics analysis of the samples.

**Table 1:** Quality control statistics of transcriptome sequencing data

| Sample Name Sample name | Original reading Raw reads | Clean readings Clean reads | Clean error rate Clean error Rate% | Q20 base proportion Q20base composition/% | Q30 base proportion Q30base composition/% |
|---|---|---|---|---|---|
| AV_1 | 20002942 | 19851348 | 0.0117 | 99.31 | 96.29 |
| AV_2 | 27149536 | 26974986 | 0.0117 | 99.34 | 96.4 |
| AV_3 | 26664328 | 26476196 | 0.0117 | 99.32 | 96.32 |
| AV_Y1_1 | 25856476 | 25688074 | 0.0117 | 99.31 | 96.32 |
| AV_Y1_2 | 20689332 | 20574560 | 0.0117 | 99.32 | 96.31 |
| AV_Y1_3 | 23582834 | 23438382 | 0.0117 | 99.34 | 96.38 |

### 3.7. Analysis of sample expression levels between groups

As shown in Figure 6, Venn diagram, the distribution of the number of molecular features between the experimental group (AV_Y1) and the control group (AV group) is as follows: there are a total of 3,777 core features in both groups; 44 specific features of the experimental group, which were not detected in the control group; There were 27 specific features in the control group, which were not detected in the experimental group. The results of the heat map of sample correlations in Figure B (characterized by $R^2$ correlation coefficients) showed that the correlation coefficients among all samples were higher than 0.95, with the correlation coefficient between AV_3 and AV_1 being 0.955 and that between AV_1 and AV_Y1_3 reaching 0.99; Hierarchical clustering results indicated that the same group of repeated samples (AV_1/2/3, AV_Y1_1/2/3) were preferentially clustered, and there was also a high degree of clustering between groups (control group and test group), suggesting that the similarity of gene expression patterns among different repeated samples was extremely high.

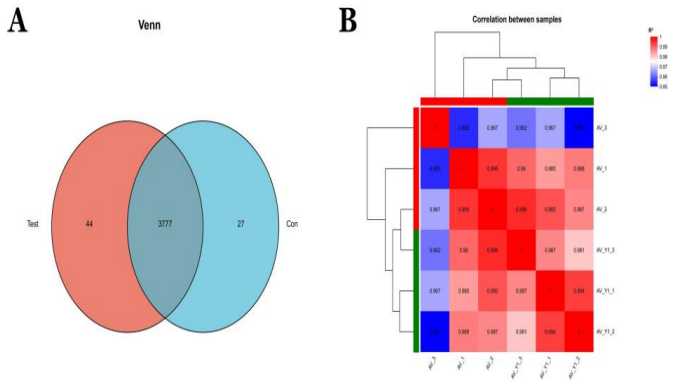


**Fig 6:** Venn diagram of expressed genes and sample correlation heatmap

### 3.8. Principal Component analysis

Principal component analysis (PCA) results indicated that PC1 and PC2 cumulatively accounted for 77.83% of the data variation (Figure 7). Samples from the control group and the test group were completely separated in the two-dimensional space of PCA, showing that the test treatment significantly altered sample characteristics, and there were essential differences between the control group and the treatment group.

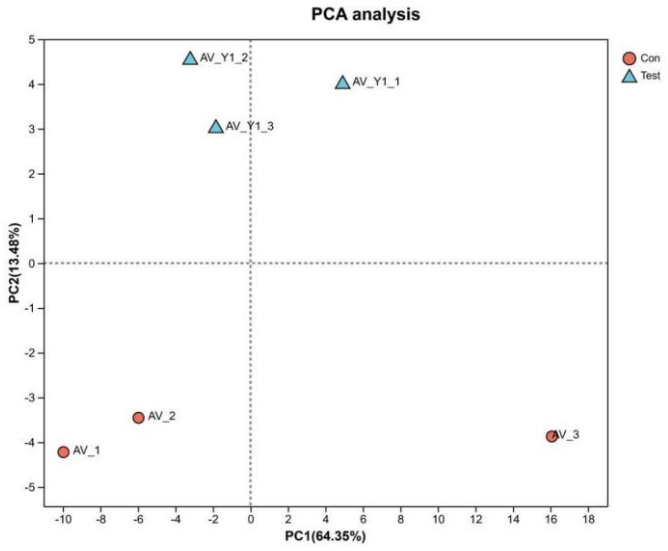


**Fig 7:** Principal component analysis (PCA) of samples from the control group (Con) and treatment group (Test).

### 3.9. Results of differential gene screening and functional annotation and enrichment analysis

Analysis was conducted using the gene differential expression analysis software DESeq2, with log2 (Foldchange)≥1 and P≤0.05 as the screening threshold. The results are shown in Figure 8A. A total of 171 genes were differentially expressed in Aeromonas verticillae after the action of verticilline, including 87 up-regulated genes and 84 down-regulated genes. The heat map of the expression patterns of the differentially expressed genes is shown in

Figure 8B. Figure 8C shows the analysis results of the GO functional annotation of the differentially expressed genes. Among them, the biological processes include biological regulation, cell killing, and tissue or biogenesis of cell components, etc. Cellular components involve cells, cellular parts, extracellular regions, etc. In addition, the molecular functions derived from enrichment analysis cover aspects such as antioxidant activity, tissue or biogenesis of cellular components, and negative regulation of biological processes. KEGG results (see Figure 8D) indicated significant changes in glycerophospholipid metabolism, PPAR signaling pathway, nucleotide metabolism, glyceride metabolism, purine metabolism, unsaturated fatty acid biosynthesis and AMPK signaling pathway after the action of coptis alkaloid, and these alterations in signaling pathways may have a major impact on cell function and survival status.

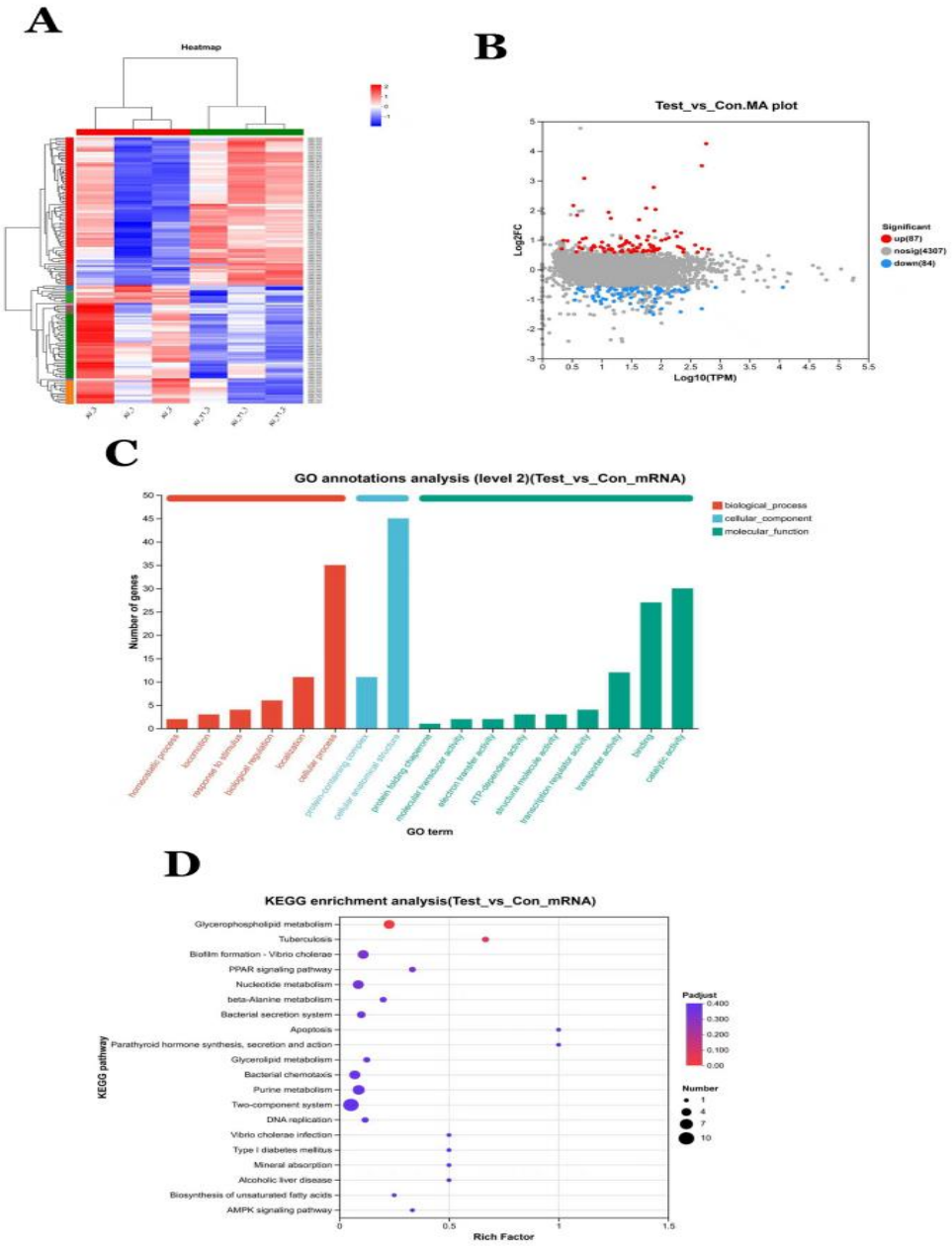


**Fig 8:** Differential gene screening, functional annotation and enrichment analysis

### 3.10. Results of RT-qPCR verification of significantly different genes in each group

To verify the accuracy of transcriptome sequencing results, three genes with significant up-regulation and down-regulation were randomly selected and verified by RT-qPCR. The results showed that the relative expression levels of *aer*, *tapA*, and *ompA* in the HLJ treatment group were extremely significantly higher than those in the CON control group ($P < 0.01$), and the expression trends were consistent with the transcriptome data, confirming the reliability of the sequencing results (Figure 9).

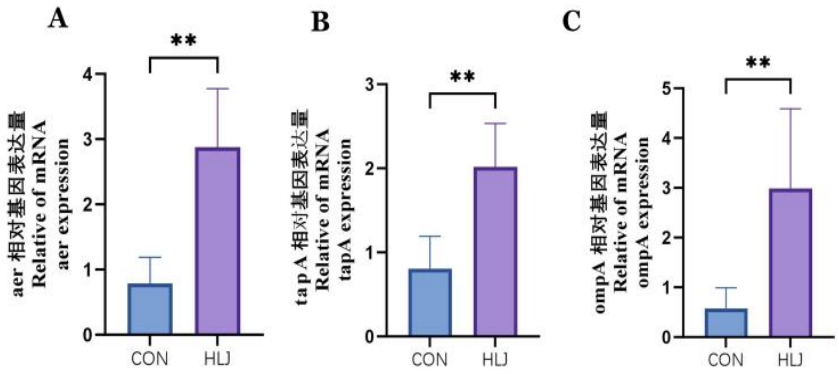


**Fig 9:** RT-qPCR verification of significantly differentially expressed genes between control (CON) and treatment (HJ) groups. * indicates significant differences between groups (P<0.05), ** indicates significant differences between groups (P<0.01).

## Discussion

This study comprehensively evaluated the antibacterial activity of coptisine against *Aeromonas veronii* and its potential mechanism of action. The results showed that coptisine had a good inhibitory effect on the pathogen, with a minimum inhibitory concentration (MIC) of 40 μg/mL. The growth curve determination further confirmed that the inhibitory effect of coptisine was significantly concentration-dependent. When the concentration reached 1 MIC, it could significantly delay the entry of bacteria into the logarithmic growth phase and inhibit their final biomass, providing a preliminary basis for its potential as an antibacterial agent.

Further investigation into the mechanism of action revealed that coptisine is likely to exert its antibacterial effect by disrupting the integrity of the bacterial cell wall and cell membrane. The extracellular release of alkaline phosphatase (AKP), an indicator of cell wall integrity, increases significantly with drug concentrations, suggesting increased permeability or structural damage to the cell wall. At the same time, the total protein content in the culture supernatant of the cells treated with coptisine also increased significantly, further supporting the loss of cell membrane barrier function, which leads to the leakage of intracellular substances. The abnormal morphology of the cells observed by transmission electron microscopy provided direct morphological evidence of this structural damage. These results collectively point to the fact that disrupting the extracellular barrier structure is a key link in the antibacterial effect of coptisine.

In addition, coptis is also effective in inhibiting the formation of *Aeromonas veronii* biofilms, and the inhibitory effect is equally concentration-dependent. Biofilms are important mechanisms of drug resistance and immune evasion in bacteria, and the inhibition of their formation may stem from two aspects: First, berberine is the most abundant alkaloid in Coptis chinensis and is a quaternary ammonium alkaloid. Berberine has a similar structure to berberine and has inhibitory[15] effects on bacteria, directly affecting their adhesion and aggregation ability; It may interfere with the quorum sensing system or extracellular polysaccharide synthesis associated with biofilm formation. Studies have shown that Coptis chinensis, *Phellodendron amurensis* and *Scutellaria baicalensis* in Huanglian Jiedu Decoction all have inhibitory effects on the biofilm of Candida albicans *in vitro*, and berberine hydrochloride also plays an important role[16] in inhibiting the formation of bacterial biofilms. This finding suggests that coptisine is not only capable of killing planktonic bacteria, but may also have the potential to combat intractable bacterial infections.

Transcriptomic analysis was conducted in this study to understand the antimicrobial molecular mechanism of coptisine from a global perspective. Enrichment analysis of the KEGG pathway in differentially expressed genes provided a strong molecular-level explanation for the phenotypic findings. Significant changes in pathways such as glycerophospholipid metabolism and unsaturated fatty acid biosynthesis are directly associated with the composition and stability of the lipid bilayer of the cell membrane. Disturbances in these pathways are likely to result in changes in membrane lipid composition, reduced fluidity, or impaired integrity, which are consistent with the observed protein leakage and AKP release. At the same time, differentially expressed genes were significantly enriched in the PPAR signaling pathway. As an important member of the nuclear receptor superfamily, PPAR has diverse functions: it participates not only in basic processes such as cell differentiation and apoptosis, but also plays a key role in the regulation of lipid metabolism and related metabolic diseases [17]. The latest research reveals that the PPAR signaling pathway plays a key regulatory role in the immune response by responding to inflammatory cytokines [18]. Perturbation of the pathway may affect bacterial lipid metabolism and cellular homeostasis, which in turn are associated with its antibacterial effects. In addition, changes in the AMPK signaling pathway are also of concern. Studies have found that AMPK plays a core regulatory role in response to cellular stress: on the one hand, it inhibits cell proliferation by suppressing the mTORC1 pathway; on the other hand, it activates autophagy [19]. Given AMPK's critical role in cellular regulation, studies have confirmed that it is an important factor influencing the progression of various diseases [20]. The alterations in the expression of genes related to this pathway in this study suggest coptisine.

It may affect the growth and adaptability of bacteria by interfering with their energy sensing and regulatory networks. Alterations in energy metabolism-related pathways such as purine and nucleotide metabolism suggest that coptisine may simultaneously interfere with bacterial energy homeostasis and biomolecular synthesis, synergistically inhibiting bacterial growth and reproduction at multiple levels. RT-qPCR validated the randomly selected differentially expressed genes, ensuring the reliability of the transcriptome data.

In the experiment, differentially expressed genes were randomly screened for RT-qPCR verification, and the results showed that the expression trends of the related genes were consistent with the transcriptome analysis, indicating that the transcriptome sequencing results were reliable and accurate. In addition, the analysis showed that compared with the control group (CON), the expression level of the tapA gene was upregulated (relative expression level increased from 0.8 to 2.0), and the expression level of the ompA gene was significantly upregulated (relative expression level increased from 0.6 to 3.0) in the coptis group. This suggests that coptisine may affect the membrane protein function or structural stability of *Aeromonas veronii* by regulating the expression of related genes such as tapA and ompA, thereby inhibiting its growth and pathogenicity.

In conclusion, coptisine exerts multi-target antibacterial effects against *Aeromonas veronii* mainly by disrupting cell wall/membrane integrity, inhibiting biofilm formation, and interfering with metabolism-related pathways. These findings support the potential of coptisine as a novel antibacterial agent for aquaculture. Further studies are needed to explore *in vivo* efficacy, molecular targets, and combined applications.

**Funding:** This work was supported by the Jingzhou Science and Technology Plan Project 2025 (2025EB21), Hubei Science and Technology Plan Project 2024 (2024EBA028), and Science and Technology Innovation Project of Hubei Provincial Department of Education (B2023537).

## References

1. Wang X, Zhuo R, Zhao Q, *et al*. Aeromonas veronii disease in aquaculture cannot be ignored. *A Guide to Getting Rich in Fisheries.* 2024;(03):61–63.
2. Shan X, Zhang H, Sun W, *et al*. Analysis of biological characteristics and protein components of extracellular products from green shrimp. *Chin Vet Med.* 2017;53(04):105–107,124.
3. Zhao Y, Shao M, Guo J, *et al*. Isolation and identification of biological characteristics of *Aeromonas veronii* from Chinese grass turtle. *Chin J Wildl.* 2022;43(02):527–532.
4. Long M, Fan H, Jiang Y, *et al*. Screening, identification and biological characteristics of two antagonistic strains of *Aeromonas* aquatic pathogen. *Fish Sci.* 2022;41(06):927–937.
5. Cheng X, Sun Z, Su Y, *et al*. Screening, identification and effect evaluation of *Aeromonas veronii* antagonistic strain J2-2. *Freshw Fish.* 2024;54(01):36–44.
6. Zhang W, Zhao J, Ma Y, *et al*. The effective components of herbal medicines used for prevention and control of fish diseases. *Fish Shellfish Immunol.* 2022;126:73–83.
7. Gou J, Li G, Lu Z, *et al*. Evaluation of the activity of extracts from different parts of Flipping white grass against common pathogenic bacteria. *Chin J Hosp Pharm.* 2024;44(11):1253–1259.
8. Sa R, Yang B, Ao C. Research overview of natural plant extracts in oxidative stress in animals. *Chin J Anim Nutr.* 2018;30(06):2021–2026.
9. Xuan Y, Zhang Y, Wei L, *et al*. Effects of adding compound Chinese herbal medicine to feed on growth and immune indicators of young rainbow trout. *Sci Fish Farming.* 2023;(10):73–74.
10. Zhang J, Zhang D, Shu D, *et al*. Effects of four traditional Chinese medicine prescriptions on antioxidant and anti-stress indices in juvenile Chinese sturgeon. *J South Agric.* 2022;53(02):568–576.
11. Elgendy MY, Ali SE, Abdelsalam M, *et al*. Onion (*Allium cepa*) improves Nile tilapia (*Oreochromis niloticus*) resistance to saprolegniasis and reduces immunosuppressive effects of cadmium. *Aquac Int.* 2023;31(3):1457–1481.
12. Li H, Guo G, Guo Z, *et al*. Effects of adding *Eucommia ulmoides* leaf powder to feed on body composition, muscle amino acid composition and physiological indicators of Yellow River carp. *Acta Hydrobiol Sin.* 2021;45(06):1222–1231.
13. Lu Q, Tang Y, Luo S, *et al*. Coptisine, the characteristic constituent from *Coptis chinensis*, exhibits significant therapeutic potential in treating cancers, metabolic and inflammatory diseases. *Am J Chin Med.* 2023;51(8):2121–2156.
14. Liu Y, Gong S, Li K, *et al*. Coptisine protects against hyperuricemic nephropathy through alleviating inflammation, oxidative stress and mitochondrial apoptosis via PI3K/Akt signaling pathway. *Biomed Pharmacother.* 2022;156:113941.
15. Bai R, Guo Y, Zhang R, *et al*. Determination of main components of *Coptis chinensis* alcohol extract and study on its antibacterial mechanism. *Adv Anim Med.* 2025;46(02):86–91.
16. Liu B, Han Q, Sheng Z, *et al*. *in vitro* intervention effects of berberine hydrochloride and coptisine on *Streptococcus suis* biofilm. *Chin Vet Med.* 2015;51(04):16–19.
17. Yoon JH, Baek SJ. Molecular targets of dietary polyphenols with anti-inflammatory properties. *Yonsei Med J.* 2005;46(5):585–596.
18. Vázquez-Carrera M, Wahli W. PPARs as key mediators in the regulation of metabolism and inflammation. *Int J Mol Sci.* 2022;23(9).
19. Hay N, Sonenberg N. Upstream and downstream of mTOR. *Genes Dev.* 2004;18(16):1926–1945.
20. Moyes KM, Drackley JK, Morin DE, *et al*. Predisposition of cows to mastitis in non-infected mammary glands: Effects of dietary-induced negative energy balance during mid-lactation on immune-related genes. *Funct Integr Genomics.* 2011;11(1):151–156.

## How to Cite This Article

Yang Z, Yang D, Pei M, Yan P, Li R, Qin M, *et al.* In vitro experiments and transcriptomic analysis reveal the antibacterial mechanism of coptisine against Aeromonas veronii. Int J Multidiscip Res Growth Eval. 2026;7(2):610–618.

## Creative Commons (CC) License